JOURNAL OF GEOPHYSICAL RESEARCH, VOL. 88, NO. A1, PAGES 295-309, JANUARY 1, 1983

EXOS-B/SIPLE STATION VLF WAVE-PARTICLE INTERACTION EXPERIMENTS
2. TRANSMITTER SIGNALS AND ASSOCIATED EMISSIONS

T. F. Bell[1], U. S. Inan[1], I. Kimura[2], H. Matsumoto[3], T. Mukai[4], and K. Hashimoto[2]

Abstract. Interactions between coherent VLF waves and energetic particles in the magnetosphere have been studied in a joint program involving the Japanese high-altitude satellite EXOS-B and the Siple Station VLF transmitter. During the period July 15 - September 7, 1979, transmissions to the EXOS-B satellite were carried out on 50 separate occasions when the spacecraft was within ±60° longitude of the magnetic field lines linking Siple Station, Antarctica (76°S, 84°W geographic, L ~ 4.1), with its conjugate station at Roberval, Canada. Of this total, 37 were carried out while the satellite was located in the 1000-1600 LT sector of the magnetosphere and 13 while in the 0300-0800 LT sector. The transmitter signals were detected on EXOS-B on 50% of the occasions when transmissions were attempted, and on 5 occasions the transmitter signals were observed to have triggered VLF emissions somewhere along their ray path between the ionosphere and the satellite. All 5 triggering events occurred in a 6-day period following a large magnetic storm that took place on August 13, 1979, with 2 events occurring in the 1130-1330 LT sector and 3 events occurring in the 0400-0600 LT sector. Analysis of the emission triggering events provided strong evidence that the triggering took place inside whistler-mode ducts and that the emissions reached the satellite only after being scattered at one end of the ducts by ionospheric irregularities. On at least one day, emissions were triggered by ducted echoes of the transmitter signals but not by the direct ducted pulses themselves. On another day a new type of triggered emission was observed. We conclude that in the noon sector of the magnetosphere the amplitude of nonducted signals from the Siple transmitter is generally less than the threshold level necessary for triggering in the nonducted mode.

Introduction

This paper reports new observations in the magnetosphere of coherent VLF waves from the Siple Station, Antarctica, transmitter (76°S, 84°W) and associated VLF emissions triggered by the transmitter signals.

[1]Radioscience Laboratory, Stanford University, Stanford, California 94305.
[2]Department of Electrical Engineering, Kyoto University, Kyoto 606, Japan.
[3]Radio Atmospheric Science Center, Kyoto University, Uji, Kyoto 611, Japan.
[4]Institute of Space and Aeronautical Science, Komamba, Tokyo 157, Japan.

Paper number 2A1577.
0148-0227/83/002A-1577$05.00

The data reported were acquired on the EXOS-B high-altitude satellite during the period July 15 - September 7, 1979, during joint VLF wave-injection experiments involving scientists from Kyoto, Tokyo, and Stanford Universities. The goal of these VLF wave-injection experiments was to acquire further understanding of interactions between coherent VLF waves and energetic particles in the magnetosphere, in particular the whistler-mode instability through which both natural and stimulated VLF emissions are produced.

Background information and references concerning the nature and origin of VLF emissions can be found in a companion article (Kimura et al., this issue), hereinafter referred to as 1. In brief, emissions are important because their existence demonstrates that coherent VLF waves can interact nonlinearly with energetic particles in the magnetosphere to strongly affect the particle energy, pitch angle, and lifetime.

A number of VLF wave-injection experiments have been carried out during the past few years with the same basic goal of understanding wave-particle interactions in the magnetosphere [Helliwell and Katsufrakis, 1974; McPherson et al., 1974; Dowden et al., 1978; Inan et al., 1977; Bell et al., 1981]. Although these experiments have revealed many new features of the emission process, simultaneous in situ energetic particle measurements were not generally available during these experiments, and thus correlations between the characteristics of the stimulated VLF emissions and the energetic particles were not obtained. In contrast, in the work reported in the present paper, simultaneous in situ measurements of both VLF wave and energetic particle characteristics were obtained on the EXOS-B satellite during each period of experimentation. Furthermore, simultaneous VLF wave data were also acquired at the three ground stations, Siple (76°S, 84°W geographic; L ~ 4.1), Roberval (48°N, 72°W geographic; L ~ 4.1), and Palmer (65°S, 64°W geographic; L ~ 2.3) during most transmissions. Thus the resultant total data sets allow a detailed description of the VLF wave environment existing at the time of the VLF wave-injection experiments.

A second unique feature of the EXOS-B/Siple Station joint wave-injection experiments is the fact that the satellite local time during transmissions was generally limited to a 2-hour interval either near noon or near dawn. Thus the local time dependence of the VLF emission process was substantially eliminated as an experimental variable, a situation that did not exist in earlier experiments [Inan et al., 1977; Bell et al., 1981] involving satellites in more eccentric orbits.

A third unique feature of the EXOS-B/Siple Station joint experiments was the fact that the satellite wave and particle data were available in real time to the experimenters. Thus a 'feed-

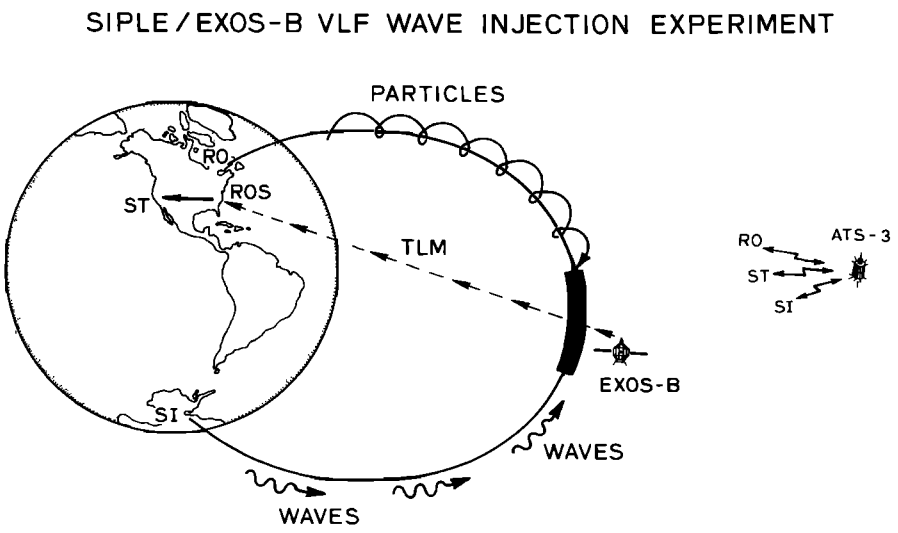

Fig. 1. Typical experimental configuration during wave-injection experiments.

back loop' could be established in which the experiment output (the wave and the particle data) could be used to generate decisions concerning the experiment input (the transmitter frequency-time function and power).

This capability of real time control of the experimental parameters based on output can greatly enhance the probability of success of in situ measurements because the VLF emission stimulation process generally exhibits a high degree of selectivity with respect to the frequency of the injected waves [Helliwell and Katsufrakis, 1974]. Often, emissions can be triggered only within a frequency band as narrow as 200 Hz. Since it is difficult at the present time to predict the triggering band for a given day and for a given L shell, access to the satellite wave data in real time eliminates the guess work associated with choosing the transmitter frequency values necessary to trigger VLF emissions.

Details of the real time mode of satellite data acquisition are shown schematically in Figure 1. Shortly before the satellite entered the transmission 'window,' an initial choice of transmitter frequency was made, based upon the presence of naturally occurring emission bands in the Siple and/or Roberval VLF data. As the satellite entered the window, VLF waves were transmitted into the magnetosphere from the Siple Station transmitter and propagated approximately parallel to the earth's magnetic field lines toward the satellite. In most cases, the satellite location was in the northern hemisphere, and thus the waves reaching the satellite had to pass through the magnetic equatorial plane, the region where the whistler-mode instability is thought to take place. The VLF wave and energetic particle data acquired on the satellite were telemetered to the NASA STADAN station at Rosman (ROS), North Carolina, where scientists were stationed to monitor the gross features of both the wave and particle data. In addition, at Rosman a 2-kHz portion of the broadband wave data, centered on the Siple transmitter frequency, was translated to the 0- to 2-kHz frequency range and relayed to Stanford University over telephone lines. At Stanford the wave data were spectrum analyzed and a rapid visual inspection of the wave spectrum was sufficient to determine if VLF emissions were being triggered by the injected waves. If this was the case, the transmitter format was usually not changed. However, if success was not achieved, the operators at Siple Station were instructed to change the frequencies of their transmissions, usually toward frequencies at which natural emission activity was observed in the satellite data.

Communication between Stanford and Siple Station was carried out via a voice link through the synchronous satellite ATS-3. Operators at Roberval Station, conjugate to Siple in Canada, were also included in the ATS-3 link so that 3-way communication was possible. Both Roberval and Siple Station were equipped with VLF spectrum analyzers so that the VLF activity at both ends of the magnetic field line linking the transmitter could be monitored visually.

Wave data from Roberval was useful in alerting the experimenters to emission triggering that might appear in the ground data but not in the satellite data. In addition, in cases in which no transmitter-induced triggered emissions or natural emission bands were present in the satellite data, the ground data were useful in displaying naturally occurring emission bands that might profitably be probed by the transmitter.

The use of this real time mode of satellite data acquisition greatly enhanced the scientific productivity of the joint EXOS-B/Siple Station wave-injection experiments.

New Results

The EXOS-B/Siple Station wave-particle interaction experiment produced the following new results:

1. Over a 7-week time span the triggering of VLF emissions by Siple transmitter pulses, or echoes of those pulses, was observed only during a 6-day period following a large magnetic storm on August 13, 1979.

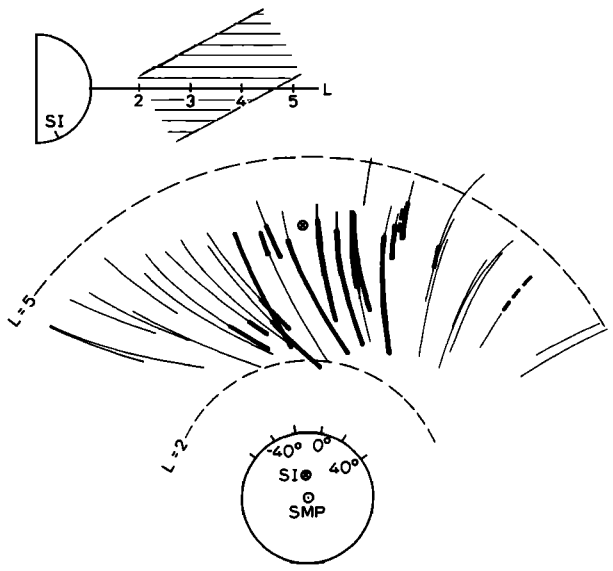

SIPLE SIGNAL RECEPTION ON EXOS-B

Fig. 2. Projection upon the magnetic equatorial plane of the portions of the EXOS-B equatorial passes on which the EXOS-B/Siple Station wave-injection experiments were carried out. Upper left-hand sketch indicates latitudinal range of orbits.

2. All triggering events appeared to take place in whistler-mode ducts, well removed from the satellite location, and the satellite emission observations apparently involved only waves that had scattered from the duct end points up to the satellite.

3. On at least one day, emissions were triggered by echoes of the transmitter pulses but not by the direct pulses.

4. During one interval of emission triggering, a new type of emission was observed in which diffuse noise bursts of more than 10-s duration were generated below the triggering pulses.

Experimental data illustrating our main findings are given below.

Observations

Distribution of Siple transmitter signals in the magnetosphere. During the period July - September 1979, Siple/EXOS-B joint VLF wave-particle interaction experiments were generally carried out whenever the EXOS-B satellite was within ±60° magnetic longitude of the Siple-Roberval Station meridian (~5°W mag.) and located on magnetic shells in the range L = 2-6. Typically, transmissions were carried out for a period of approximately 1 hour while the satellite was located within this 'window,' which was chosen on the basis of previous wave-injection experiments [Inan et al., 1977; Bell et al., 1981].

Transmissions were carried out on 50 separate occasions, with 37 transmissions occurring during near-equatorial (inbound) passes and 13 during high-latitude (outbound) passes. The local time of the satellite lay in the approximate range 1000-1600 LT for the equatorial passes and 0300-0800 LT for the high-latitude passes.

Figure 2 shows a projection upon the magnetic equatorial plane of the portions of the EXOS-B equatorial passes on which the EXOS-B/Siple experiments were carried out. The orbital sections along which transmitter signals were detected on the satellite are denoted by thick lines, either continuous or dashed. The latitudinal range of orbits, projected upon the Siple-Roberval magnetic meridian, is shown in the upper left corner of the figure. The intersection with the magnetic equatorial plane of the Siple-Roberval Station magnetic field line is shown by a circled 'X' in the figure. As shown in the figure, in most cases the transmitter signals were detectable only on those inbound passes that lay within ±30° magnetic longitude of the transmitter meridian. However, a notable exception to this rule occurred on August 15, 1979, when Siple signals were observed approximately 40° east of the Siple-Roberval meridian.

The portions of the equatorial passes on which Siple transmitter signals were observed to trigger VLF emissions, are shown by dashed thickened lines in the figure. Of the 37 transmissions carried out during equatorial passes, 19 were detected in whole or in part by the satellite, and of these 19, 2 were associated with triggered emissions. Thus while the rough probability of detecting Siple transmitter signals on orbits within the experimental window was approximately 50%, the probability of observing transmitter signals associated with triggered VLF emissions was approximately 5%. These probabilities are in agreement with the results

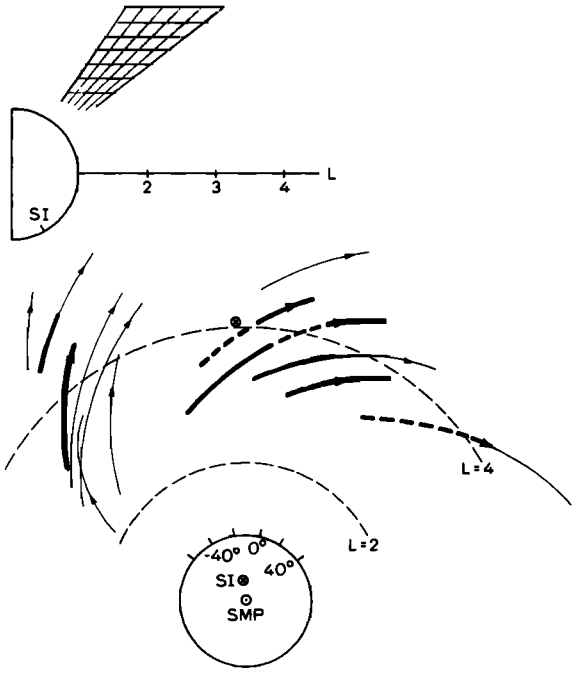

SIPLE SIGNAL RECEPTION ON EXOS-B

Fig. 3. Projection upon the magnetic equatorial plane of the EXOS-B high latitude passes on which the EXOS-B/Siple Station wave-injection experiments were carried out. Upper left-hand sketch indicates latitudinal range of orbits.

TABLE 1. Relevant Whistler Characteristics During Period August 14-19

Date	f_N kHz	t_N s	t_S s	L Shell	N_O cm^{-3}
Aug. 14 ~0800 UT	9.3 ± 0.7	0.8 ± 0.05	1.0 ± 0.05	3.3 ± 0.1	~300
Aug. 15 ~1400 UT	5-4(W_2) 15-8(W_1)	1-1.5(W_2) 0.7-1.2(W_1)	1.2-1.7(W_2) 1-1.4(W_1)	4.0-4.3(W_2) 2.8-3.4(W_1)	100(W_2) 600-1000(W_1)
Aug. 17 ~0900 UT	4.3 ± 0.2	2.0 ± 0.1	2.1 ± 0.1	4.2 ± 0.1	~300
Aug. 18 ~1000 UT	4.5 ± 0.1	2.1 ± 0.1	2.3 ± 0.1	4.1 ± 0.1	~400
Aug. 19 ~1700 UT	9 ± 0.5	1.5 ± 0.15	1.6 ± 0.05	3.3 ± 0.1	~1000

of previous wave-injection experiments involving the Siple transmitter and the Explorer 45, the IMP 6, and the ISEE 1 satellites [Inan et al., 1978; Bell et al., 1981].

Figure 3 shows a projection upon the magnetic equatorial plane of the 13 high-latitude passes during which transmissions were carried out. The format of this figure is identical to that of Figure 2. It can be seen that the satellite was located at higher geomagnetic latitudes (38° - 58°N) during each outbound pass, and that reception of Siple signals occurred over a wider range of geomagnetic longitudes (65°W - 40°E) than in the case of the inbound equatorial orbits (35°W - 35°E).

Siple signals were detected on portions of 6 of the high-latitude orbits, and the rough probability of detecting the Siple transmissions was approximately 46%. However, 3 of the 6 periods of detection were associated with VLF emissions triggered by the Siple signals and thus the probability of observing transmitter signals associated with triggered VLF emissions was 23% on the high-latitude passes, a value approximately 4 times that of the equatorial passes.

The apparent higher probability of triggering in the dawn sector may be the result of generalizing from a small number of samples. On the other hand, the results from an earlier study [Bell et al., 1981] indicate that emission triggering tends to peak in the dawn sector for other VLF transmitters.

It is interesting to note that out of 50 passes, VLF emissions were seen to be triggered by Siple signals only during a 6-day period following a large magnetic storm (Kp = 7+) on August 13, 1979. This finding suggests that the recovery period following large magnetic storms is a very favorable time for observing VLF wave growth and emission triggering in both the noon and dawn sectors.

Siple signal characteristics. A single transmission format was used during the Siple/EXOS-B wave-injection experiments, which consisted of a series of fixed-frequency pulses of variable duration, as well as variable-frequency 'ramps' of both positive and negative slope. This format occupied a 1-kHz bandwidth centered on a frequency f_c, which was chosen after review of the natural wave activity detected at Siple and Roberval Stations and on the EXOS-B satellite at a time shortly before the transmissions were to begin. In each case, the transmitting antenna was tuned to the frequency f_c, and maximum input power, usually exceeding 100 kW, was delivered to the antenna at that frequency. Power delivered at $f_c \pm 500$ Hz was generally in the range 50-70 kW, depending upon the value of f_c. The radiated power at f_c lay in the range 1-2 kW during the experiments. The transmitting format of EXOS-B resembled closely that which has been used in earlier wave-injection experiments involving the ISEE 1 satellite [Bell et al., 1981].

During periods of Siple signal reception, the S/N ratio of the detected signals was usually high enough so that accurate measurements of the wave amplitude could in principle have been obtained. However, the absolute level of the signals and accompanying background noise was sometimes high enough to overload the receiver, causing clipping to occur. In these cases only a lower bound on the signal amplitude could be obtained. Thus the only accurate amplitude measurements were those made of the lower-amplitude transmitter signals.

In most cases the gross characteristics of the Siple signals, such as time delay and S/N ratio, were similar to those reported in earlier wave-injection experiments [Inan et al., 1977; Bell et al., 1981]. However, a number of new features of the emission triggering phenomenon were discovered during the present experiment. Details of these features are given below.

VLF emissions triggered by Siple transmitter signals. Siple transmitter signals were observed to trigger VLF emissions on 5 separate orbits during the EXOS-B/Siple wave-injection experiments. Observations of these artificially stimulated emissions (ASE) were confined to a 6-day period, August 14-19, which followed a major magnetic storm (Kp ~ 7+) on August 13.

Three of the periods in which ASEs were observed occurred during high-latitude passes and two during equatorial passes. Table 2 in paper 1 summarizes a few significant details concerning the satellite passes during which ASE activity was observed.

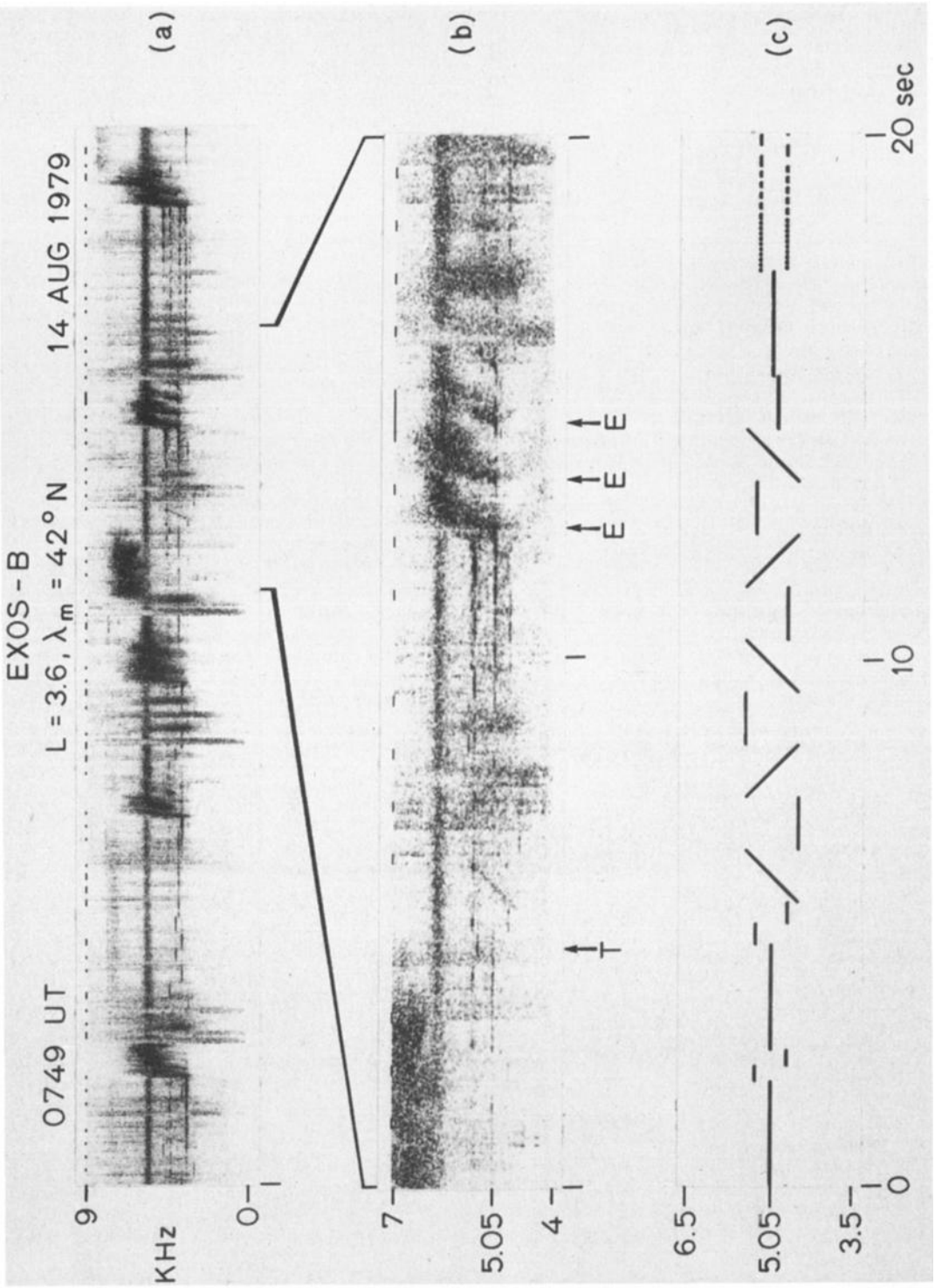

Fig. 4. Sample of the broadband VLF spectrum acquired on EXOS-B on August 14, 1979. (a) An 80-s display of the VLF spectrum in 0-to-9 kHz range during triggering events. (b) High time resolution spectrogram of 20-s portion of panel a. (c) Transmitter format associated with panel b.

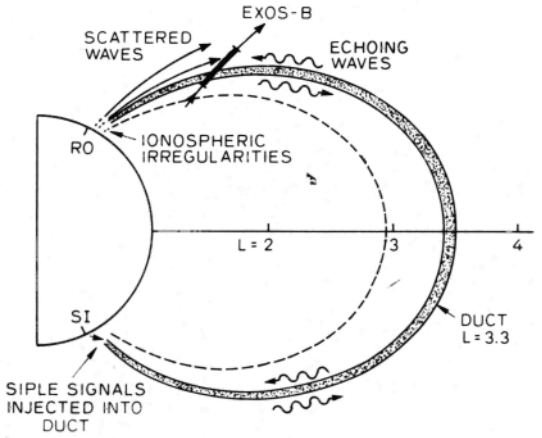

Fig. 5. Possible mode of propagation of Siple signals to the EXOS-B satellite on August 14, 1979, near 0750 UT. The echoing waves consist of Siple signals that are trapped in the duct at L ~ 3.3. The scattered waves consist of Siple signals that have been scattered from the duct by ionospheric irregularities and then propagate to the satellite in a nonducted mode. The portion of the satellite orbit over which emission triggering was observed is indicated by a thickened line. Although the satellite track passes through the same L shell as that of the duct, there is no evidence that the satellite was actually within the duct at any time.

On each pass there was strong evidence that the observed ASEs were triggered in whistler-mode ducts by Siple pulses, or echoes of those pulses, which were propagating along the ducts between conjugate hemispheres.

A good part of this evidence is based upon characteristics of ducted whistlers that were observed at ground stations during the times of ASE activity on each of the 5 passes.

Table 1 summarizes some significant details concerning those whistlers. Column 1 gives the time of the pass; column 2 gives the nose frequency f_N of each whistler trace, as measured or calculated; column 3 gives the time delay t_N of each whistler at f_N; column 4 gives the group time delay at 5 kHz of each whistler; column 5 gives the inferred L shell location of the duct associated with each whistler trace; and column 6 gives the inferred equatorial electron density N_o associated with each duct. The values of L and N_o for each duct were calculated by the whistler method, using a standard diffusive equilibrium model for the cold plasma density [Inan et al., 1977; Bell et al., 1981]. In cases in which f_N was not measurable, its value was calculated by using the method of Bernard [1973].

Although ASE associated with direct transmitter pulses have been observed on satellites in earlier wave-injection experiments [Inan et al., 1978; Bell et al., 1981], satellite observations of emission triggering by echoes of transmitter pulses have not previously been reported. Results of the present experiment are unusual in that, on at least one day, echoes of the transmitter pulses triggered VLF emissions, while the direct pulses themselves did not.

Evidence for this effect was acquired on the August 14 satellite pass, a portion of the data from which is shown in Figure 4. Panel a shows the wave spectrum in the 0-9 kHz range starting at 0749 UT. Panel b shows a high time resolution spectrogram of a portion of panel a. Panel c shows the transmitter format associated with

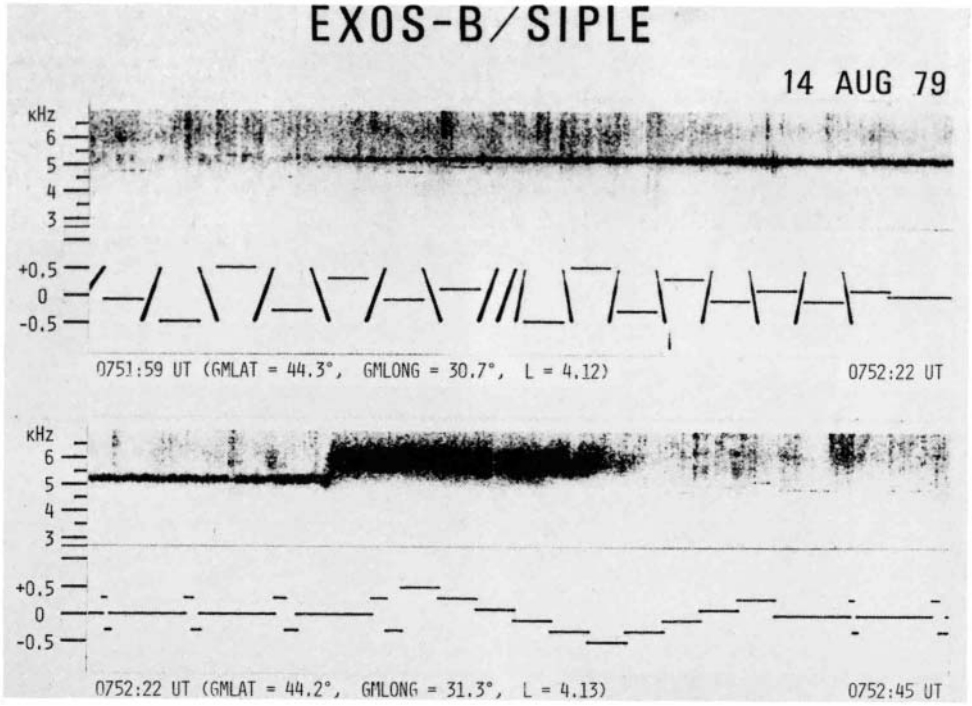

Fig. 6. Example of apparent catalytic action of Siple signals in natural emission events. Intense narrowband emission near 5.4 kHz begins to form at approximately 0752:05 UT. A few seconds after center frequency of noise band intersects Siple transmission frequency, strong burst of emissions is triggered from noise band.

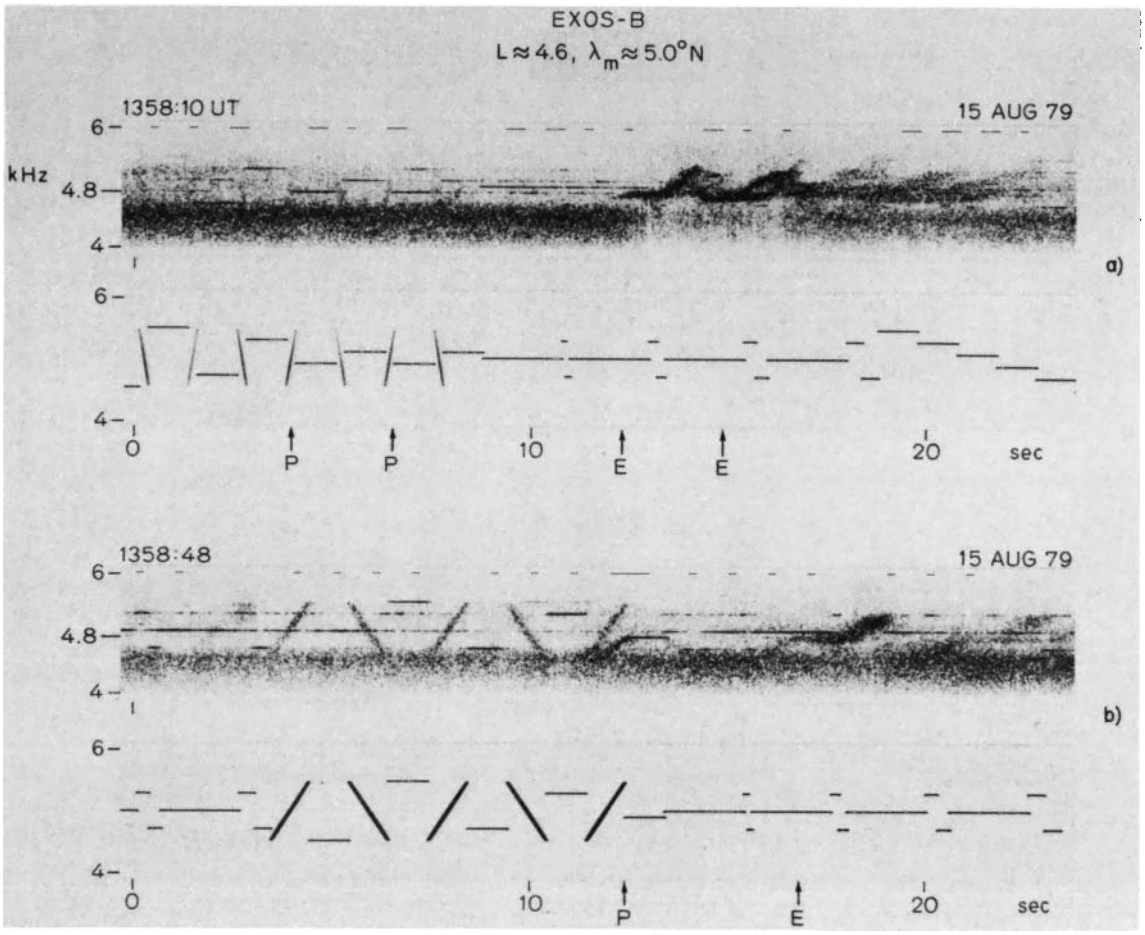

Fig. 7. Examples of VLF wave spectrum on EXOS-B during triggering events. (a) Rising emissions apparently triggered by echoes of pulses at 4.8 kHz. (b) Rising emissions apparently triggered by echoes of pulse at 4.8 kHz.

panel b, shifted forward in time by 1.1 s to correct for the wave propagation delay to the satellite at 5.05 kHz.

In panel b, the first 2 pulses at 5.05 kHz are each 2 s in duration. Following the termination of the second pulse at time T, no further pulses occur at 5.05 kHz for 10.4 s.

It can be seen that the first 2 CW pulses at 5.05 kHz are received on the satellite with a rather low S/N ratio and that no VLF emissions are associated with these pulses. However, approximately 5 s after termination of the last pulse at 5.05 kHz, echoes of the original 2 pulses begin to arrive at the satellite and these echoes are clearly associated with groups of strong rising-frequency VLF emissions (marked by 'E' on time axis).

Analysis of whistler data received at Siple and at Palmer Station close to the time of transmission to EXOS-B on August 14 showed the presence of a whistler duct near L = 3.3 with a group delay time at 5.05 kHz of approximately 1.0 s.

During the period that the Siple transmitter pulses were observed on the satellite the group propagation time at 5.05 kHz remained relatively constant at 1.0 ± 0.1 s, even though the satellite moved continually to higher magnetic shells.

A constant propagation time of this value would be consistent with a model in which the transmitter pulses propagate into the northern hemisphere in the whistler-mode duct located at L = 3.3. Upon reaching the ionosphere over Roberval, a portion of the wave energy is scattered upward to the satellite by density irregularities. The portion of the wave energy reflected back into the duct continues to echo, and additional wave energy is scattered up to the satellite each time an echo arrives in the ionosphere near Roberval. This mode of propagation is illustrated in Figure 5.

In addition to the events in which echoes of Siple signals were observed to trigger VLF emissions directly, there were a number of cases in which the Siple signals (and/or echoes) appeared to act as a catalyst in natural triggering events. An example of this behavior is shown in Figure 6. It can be seen in the figure that at approximately 0752:05 UT a strong narrow band (~100 Hz) noise begins to form near 5.4 kHz. Initially this noise band lies between transmitter frequencies and apparently is not associated with either direct Siple signals or echoes. However, the lower cutoff frequency of the noise band decreases slowly as the bandwidth of the noise increases, until by 0752:25 UT the center frequency of the noise band is located at 5.35 kHz, one of the frequencies at which pulses were transmitted at that time. A few seconds after this condition prevailed, a strong VLF emission was triggered from the noise band. Further discussion of the event of Figure 6 can be found

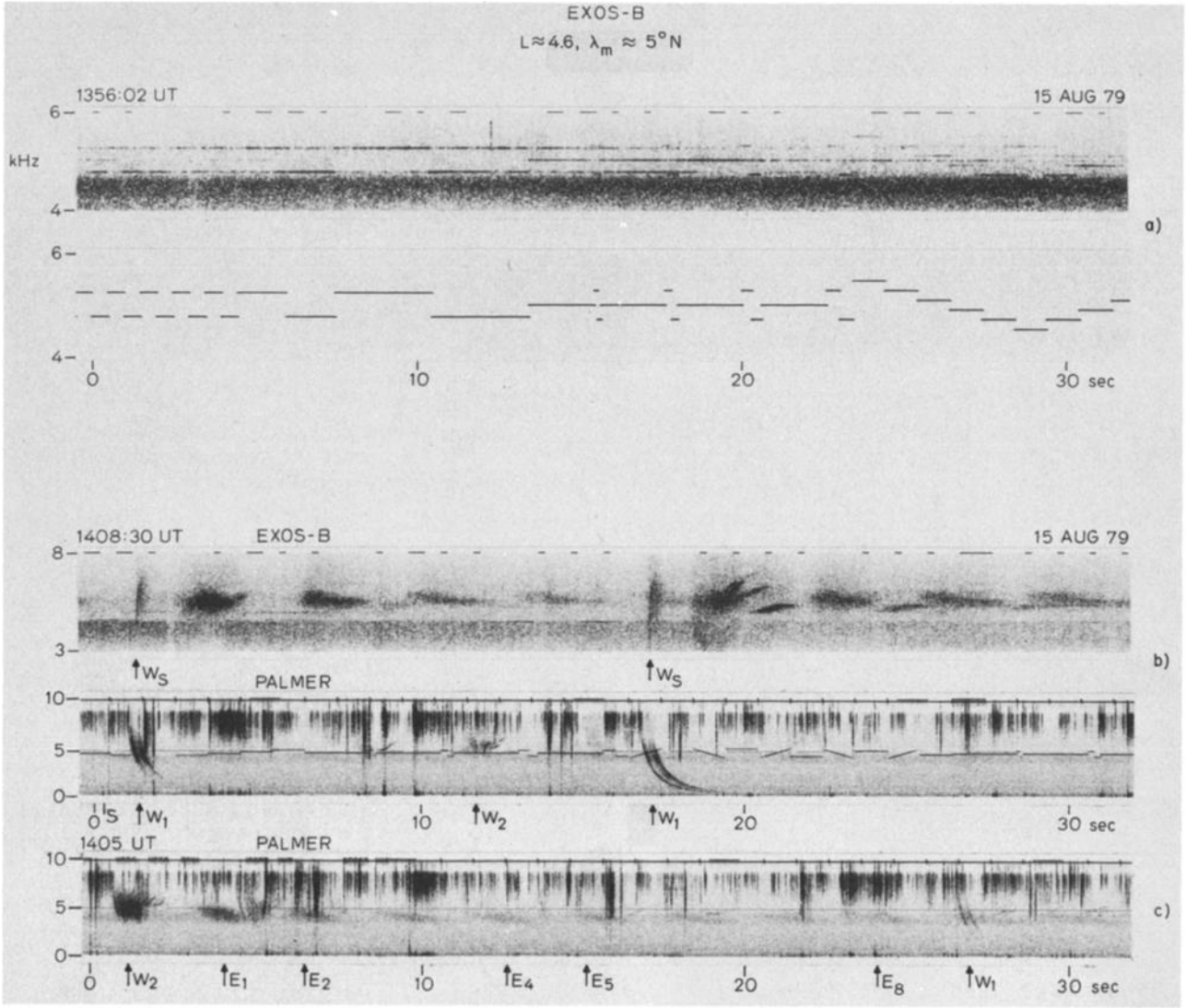

Fig. 8. (a) EXOS-B wave spectrum at time just preceeding onset of triggering. Echoing effects are very prominent. (b) Simultaneous EXOS-B and Palmer Station wave spectrums. W_1 whistler groups observed at Palmer are associated with W_S whistlers observed on EXOS-B. W_2 whistlers have no counterpart in the satellite data. (c) Most whistlers in W_2 group are accompanied by VLF emissions triggered near the upper cutoff frequency of each whistler trace. W_2 whistlers subsequently echo between hemispheres with period of approximately 2.5 s. The first 3 echoes are indictaed (E_1, E_2, E_3). At least 8 echoes (E_8) can be seen. A weak W_1 group can be seen at approximately the 27-s mark.

in Kimura et al., [1981]. This type of catalytic interaction may be similar to that reported for power line radiation [Park and Helliwell, 1978].

Data acquired on EXOS-B on August 15 form a second set in which echoes of pulses from the Siple transmitter appeared to be involved in triggering VLF emissions while the direct pulses did not.

Figure 7 shows examples of the VLF wave spectrum during the time that ASEs were observed to accompany the transmitter signals. Shown below each spectrogram is the transmitter format shifted forward in time by 1.8 s to compensate for the group delay between the transmitter and the satellite of the first arriving signals. This very large value of group time delay suggests that the first arriving signals have propagated in a nonducted mode from the ground to the satellite. During the period of triggering, there were no clear instances in which direct nonducted signals from the transmitter were observed to trigger VLF emissions, but instead there were a number of instances in which it appeared that signals on longer time-delay paths were triggering emissions. For instance, the upper panel of Figure 7a shows a case in which a set of rising emissions, beginning near the 13- and 15-s marks, appear to be triggered from the wave train (at the same frequency) following two 1-s long pulses at 4.8 kHz that begin near the 4- and 7-s marks. Another example of this behavior is shown in the upper panel of Figure 7b, where a rising emission near the 17-s mark (see arrow labeled 'E' on time axis) appears to be triggered from the wave train following a 1-s long pulse at 4.8 kHz located near the 12.5-s mark (see arrow labeled 'P' on time axis).

Since the wave trains that follow the direct nonducted pulses endure for 2-5 s (at the time

shown), there is good reason to believe that at least some of the components in the wave train represent energy echoing in a duct. This hypothesis is supported by the characteristics of the wave spectrum shortly before triggering was initiated. For instance Figure 8a shows the wave spectrum at 1356 UT, approximately 1 min before the onset of the emission triggering. The bottom panel of Figure 8a shows the associated transmitter format. Comparison of the two panels shows that echoing effects are very prominent, with many of the individual pulses being extended by as much as 7 s beyond their transmitted length.

For a dipole magnetic field model, the local electron gyrofrequency f_H at the satellite would have been approximately 9 kHz at 1358 UT. Since local wave guidance in whistler-mode ducts is possible only for $f \leq f_{H/2}$, it is clear that the echoing seen in Figure 8a is not occurring in a duct near the satellite location. Furthermore, ray tracing studies show that for commonly accepted models of the cold plasma distribution in the magnetosphere, waves for which $4.5 \leq f \leq 5.5$ kHz cannot echo in a nonducted mode near $L \sim 4.6$. Consequently, a portion of the longer time delay signals seen on the satellite most probably echoed on a lower L shell and reached the satellite only after having been scattered from the lower shell.

Simultaneous wave data from EXOS-B and Palmer Station, a portion of which is shown in Figure 8b, showed that noise busts triggered by ducted whistlers had echoed in a duct below $L \sim 4.6$ and subsequently were scattered from the duct to the satellite location. The simultaneous wave data further indicated that at least two groups of ducts were involved in guiding whistlers: whistlers propagating along one set of ducts W_1 being primarily confined to lower L shells ($L \sim 3$), and whistlers in the second set of ducts W_2 being primarily confined to higher L shells ($L \sim 4.5$). Examples of these two types of whistlers are shown in the lower panel of Figure 8b.

As described in the appendix, the complete set of ground and satellite data suggests a model in which signals from the transmitter are originally injected into both ducted and nonducted modes near the transmitter location at $L \sim 4$. A portion of the nonducted signal energy propagates directly to the satellite near $L \sim 4.6$ and arrives with a group time delay of ~1.8 s. The ducted portions of the transmitter signals propagate toward the northern hemisphere in one or more whistler ducts, reflect in the northern hemisphere and propagate back into the southern hemisphere. Upon reaching the duct end point in the south, a small portion of the signal energy is scattered by ionospheric irregularities up to the satellite location. However, the major portion of the signal energy reflects in the ionosphere, reenters the duct, and echoes between hemispheres, with additional scattering taking place each time the echoing wave packets encounter the irregularities in the southern ionosphere. A sketch of the model we propose is shown in Figure 9.

In our model, the wave train that follows each direct nonducted transmitter pulse is made up of contributions from a number of closely spaced ducts near $L \sim 4$. The waves from each duct consist of two-hop and higher-order even-hop echoes of the transmitted signals.

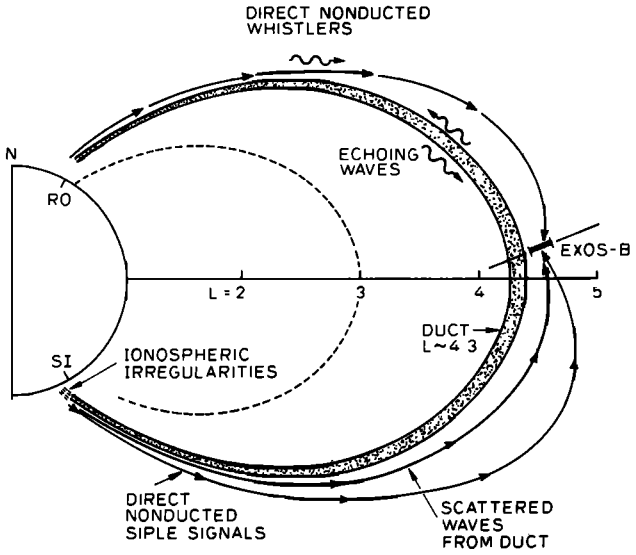

Fig. 9. Possible modes of propagation of Siple signals and whistlers to the EXOS-B satellite on August 15, 1979, near 1400 UT. The echoing waves in the duct at $L \sim 4.3$ consist of whistlers and Siple signals with a two-hop time delay of approximately 3.4 s. The time delay to the satellite of the direct nonducted Siple signals at 5.05 kHz was approximately 1.8 s, and the time delay of the direct nonducted whistlers from the north was 1.3 s at 5.05 kHz. The scattered waves from the south consisted of echoing whistlers and Siple signals scattered from the duct at $L \sim 4.3$.

As is shown in the appendix, the time delays between the beginning of the wave train and the associated emissions are such that it is probable that some of the ASEs were triggered not by a direct ducted pulse as it propagated into the north but by echoes of this pulse propagating either into the north or south.

In the above we have presented data in which echoes of Siple signals were observed to trigger VLF emissions, while the direct pulses did not always do so. This situation was reversed in the data acquired on August 17, where only the direct transmitter signals were observed to trigger emissions.

Examples of the broadband VLF wave spectrum during the period of emission triggering are shown in Figure 10. The upper panel of this figure shows the VLF spectrum for the 0-8 kHz wave band of the EXOS-B receiver over a 2-min interval. The lower panel shows 2 sections of the wave data with higher frequency and time resolution, and also shows directly below these 2 sections the transmitter format appropriate to each interval, shifted forward in time to correct for the wave propagation delay of approximately 2.4 s. The signals transmitted from Siple Station at this time lay in the band 5.05 ± 0.5 kHz. It can be seen in Figure 10 that beginning at 0930 UT, the natural VLF background noise is strongly suppressed whenever the transmitter pulses are present in the receiver. This

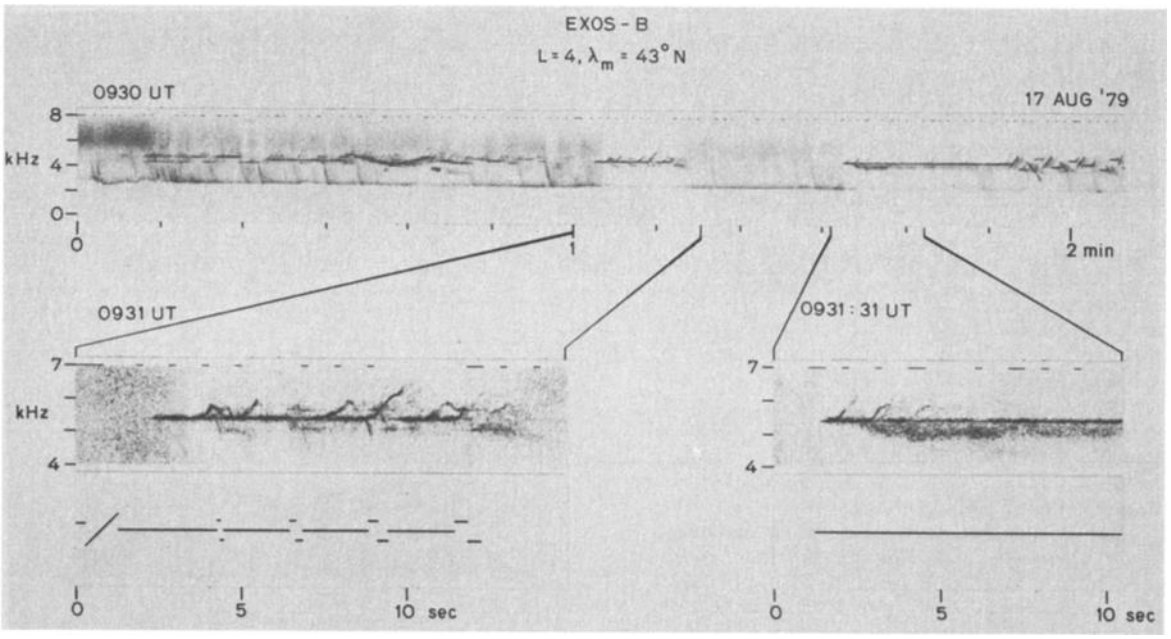

Fig. 10. Examples of the broadband VLF wave spectrum received on EXOS-B on August 17, 1979. The upper panel shows the 0-to-8 kHz band of the receiver over a 2-min interval when emission triggering was observed. The lower panel shows selected portions of the data with higher resolution in frequency and time.

suppression results from the fact that the transmitter signal strength exceeds the linear dynamic range of the receiver, thus producing an effect similar to automatic gain control.

The suppression effect clearly demonstrates the fact that the transmitter signals and associated VLF emissions were by far the strongest signals in the 0- to 8-kHz band at this time. However, since the receiver was in saturation, no measure of the absolute amplitude of the transmitter pulses could be obtained, although a lower boundary of 2.8 μv/m (the saturation level) can be inferred.

During the 2-min period shown in Figure 10, every pulse greater than 500 ms in length triggered one or more VLF emissions, including rising and falling tones and hooks. This high level of emission activity stands in strong contrast to that of August 14 and 15 in which only a small percentage of the transmitter pulses and/or echoes were associated with emissions. In most respects, the emissions in Figure 10 closely resemble those triggered by ducted waves and detected at ground stations [Helliwell and Katsufrakis, 1974]. However, one unusual feature of the data is the diffuse noise bursts that were often seen to be triggered below the input wave frequency. A good example of this phenomenon occurs at approximately 0931:33 UT. This type of hisslike emission has never previously been observed to be triggered below the input wave frequency, although similar noise bands of shorter duration have occasionally been observed to be triggered above the input wave frequency [Bell et al., 1981].

Analysis of whistler data acquired at Siple and Palmer Stations, close to the time of transmissions to EXOS-B, shows the presence of a whistler-mode duct located near L = 4.2. The one-hop time delay at 5.05 kHz of whistlers propagating in this duct was 2.1 ± 0.05 s. No data were available at Roberval during the time that ASEs were observed on the satellite. However, the one-hop time delay of ducted Siple transmitter signals observed at Roberval at 0935 UT was 2.1 ± 0.1 s at 5.05 kHz, and at this time, and previously, the ducted signals were accompanied by ASEs. From this information we infer that the Siple transmitter signals propagated to Roberval along the duct at L = 4.2.

The time delay of Siple transmissions at 5.05 kHz as observed on EXOS-B during the emission triggering event varied from 2.4 ± 0.1 s at 0930 UT to 2.7 ± 0.1 s at 0934 UT. Thus the transmitter signals were detected at Roberval before they were detected on the satellite.

On the basis of these data we infer that the triggered emissions observed on August 17 were actually triggered in the whistler-mode duct located at L = 4.2 and propagated to the satellite only after reflection or scattering in the upper ionosphere near Roberval. For this case the mode of propagation would be very similar to that shown in Figure 5.

Emission triggering associated with direct Siple transmitter pulses was also observed on August 18 and 19. However, the S/N ratio of the transmitter signals and triggered emissions was quite low and the characteristics of these signals were difficult to measure precisely. Nevertheless, on August 18, analysis of satellite data and whistler data acquired at Siple and Palmer Stations close to the time of transmission to EXOS-B demonstrated the strong possibility that the transmitter signals and associated VLF emissions had propagated into the northern hemisphere along a duct near L = 4.1 and then scattered from the lower ionosphere up to the satellite. The propagation mode for this case would resemble that of Figure 5.

Emission triggering by Siple transmitter pulses on August 19 was observed on EXOS-b only

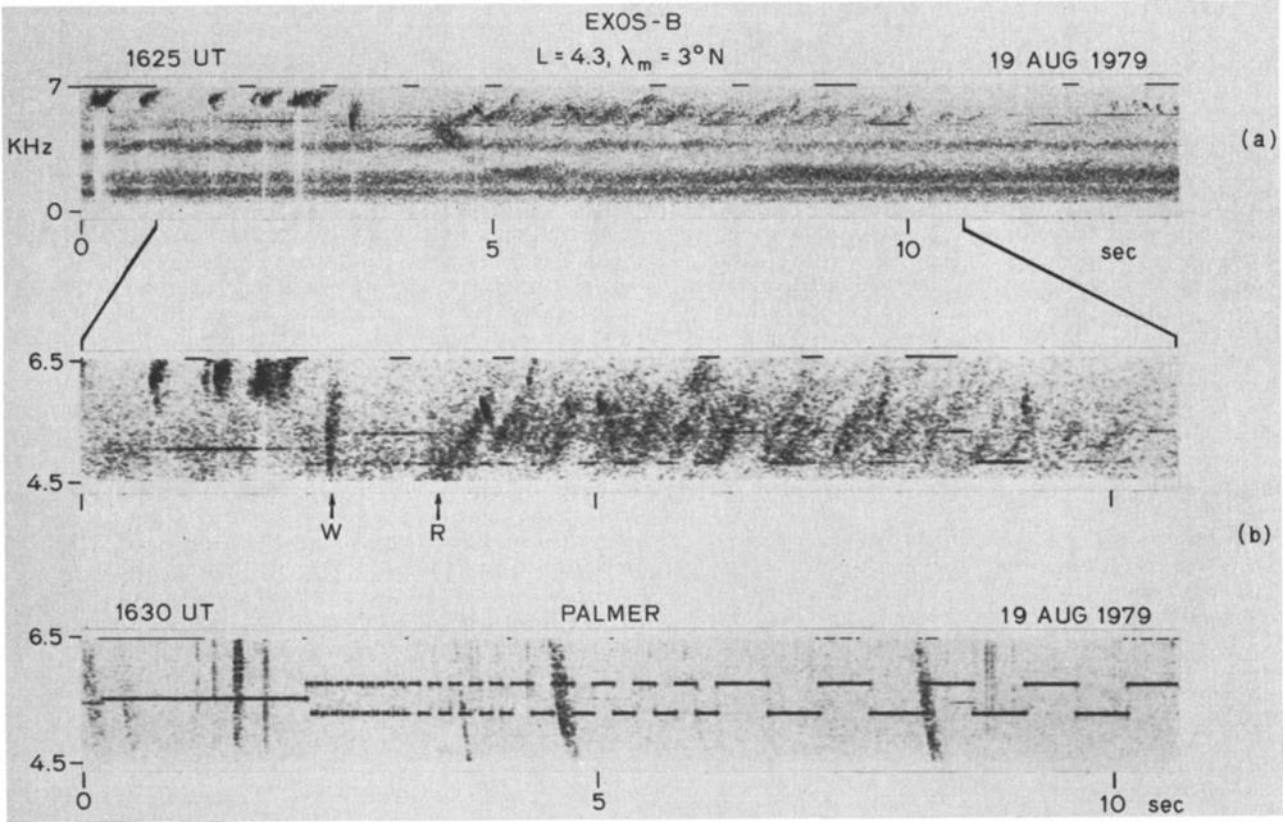

Fig. 11. Portion of the VLF wave spectrum received by EXOS-B on August 19, 1979. (a) Wave spectrum in 0-to-7 kHz band during entrainment event. (b) Higher time and frequency resolution spectrograms.

during a 10-s period near 1705 UT in which the satellite was located near L = 3.3 and $\lambda_m \sim 5°S$. However, for 15 min preceeding the satellite events, ASEs and associated Siple transmitter signals had been observed at Roberval on a one-hop path, and at Palmer the echo of the Roberval signals could be observed. Thus during the 10-s interval ASEs were observed simultaneously on EXOS-B and at Roberval and Palmer Stations.

Analysis of simultaneous ground and satellite data suggested a model in which the transmitter signals triggered VLF emissions while propagating into the northern hemisphere along a duct near L = 3.3 that was removed in longitude from the satellite location. A portion of the ducted signal then scattered from irregularities near the duct end point in the northern hemisphere and propagated in a nonducted mode up to the satellite. For this case the mode of propagation would be analogous to that shown in Figure 9, with the exception that scattering would take place in the north and the direct nonducted signals would be absent.

Another interesting event observed on August 19 was a probable 'entrainment' interaction in which Siple transmitter pulses apparently entrained a series of emissions, the first of which was triggered by a whistler. The entrainment event is illustrated in Figure 11. Panel a in this figure shows the satellite wave spectrum in the band 0-7 kHz. The upper section of panel b shows a portion of the wave spectrum of panel a at higher frequency resolution. The transmitter format in use at this time (1625 UT) was identical to that shown in the lower section of panel b. The activity begins with the arrival of a whistler close to the 2.5-s mark (exact point denoted by arrow labeled 'W' on time axis). The first echo of this whistler triggers a rising-tone VLF emission whose arrival (at 4.5 kHz) is denoted by an arrow labeled 'R' on the time axis. The first emission is followed by numerous additional emissions which appear to be triggered by the variable-length transmitter pulses at 4.8 kHz. The fact that the main triggering only begins after the arrival of a whistler-triggered emission suggest that the event may actually be an entrainment process [Helliwell and Katsufrakis, 1974] in which a group of whistler-triggered emissions are entrained by the transmitter pulses at 4.8 kHz. Entrainment is a common feature of the VLF process, as observed at ground stations, and occurs under a wide variety of conditions [Helliwell and Katsufrakis, 1974; Inan et al., 1977]. However, this type of event is rarely seen in satellite data, and the process itself is not well understood.

At 1625 UT, the transmitter signal time delay to the satellite was approximately 2 s. If these signals had been ducted, we would expect a one-hop signal time delay of approximately 2.4 s at ~5 kHz on the L shell of the satellite. However, whistler data from Siple, Palmer, and Roberval Stations show that the one-hop time delay at 5 kHz on ducts near L ~ 4.3 was ~1 s at this time. Thus, we conclude that it is very likely that the Siple transmitter signals shown in Figure 11 propagated to the satellite in a nonducted mode.

No other events similar to that of Figure 11 were observed on August 19.

Discussion and Conclusions

For reasons given above, we conclude that the VLF triggered emission data of August 14, 15, 17, 18, and 19 can be explained by a model in which emissions are triggered by transmitter signals, and/or echoes of these signals, which are propagating in a whistler-mode duct, and these signals and associated emissions are subsequently scattered from a duct end point up to the satellite location. Thus, only the apparent entrainment event of August 19 appears to involve interaction between nonducted transmitter signals and energetic particles.

This apparent inability of nonducted Siple transmitter signals to trigger VLF emissions does not appear to stem from unusual conditions in the magnetosphere. For example, during the period July 15 - September 7, ducted transmitter signals and associated VLF emissions were observed at Roberval on roughly 20% of the days when transmissions were carried out (12 out of 55). This probability is comparable to the 30% detection rate obtained for similar wave-injection experiments carried out from Siple Station in the period July-August, 1973 [Carpenter and Miller, 1976].

On the basis of these findings we conclude that nonducted VLF signals from the Siple Station transmitter are unlikely to trigger VLF emissions in the noon-afternoon sector of the magnetosphere, even in periods when ducted signal components are triggering vigorously.

This circumstance may also be true for transmissions in the dawn sector, but the smaller number of transmissions in this sector (12 cases) make such a conclusion less defensible.

Our results suggest that in the noon-afternoon sector the amplitude of Siple transmitter signals is below the threshold necessary for triggering. Evidence for this effect is demonstrated by the general ability of nonducted signals from the Omega VLF navigational transmitter in North Dakota to trigger VLF emissions in the magnetosphere under a wide range of magnetic disturbance ($0 \leq Kp \leq 4$) [Bell et al., 1981]. This difference in triggering ability may be primarily due to the higher output power of the North Dakota Omega transmitter, which at 10 kW is approximately 10 dB more than that of the Siple Station transmitter. For instance, if the triggering process for nonducted waves has an amplitude threshold [Helliwell et al., 1980] below which triggering will not occur and if this threshold depends upon the background noise level in the plasma, then it can be expected that nonducted signals of generally higher amplitude would be more likely to trigger emissions.

Other factors that may be involved in determining the relative triggering ability of these two transmitters are the different transmitter locations ($L \sim 3.5$ for the Omega transmitter; $L \sim 4.1$ for the Siple transmitter), the different operating frequencies (10.2-13.6 for Omega, usually 3-6 kHz for Siple), and the different local times of transmissions.

One of the unique features of the EXOS-B data is the fact that on at least one day, August 14, emission triggering was associated with echoes of the direct Siple pulses but not with the direct pulses themselves.

This type of behavior has been noted previously in natural triggering events, but has not been reported to have occurred in previous wave-injection experiments. One possible explanation for the effect in the Siple Station signals involves the existence of a region of wave growth near the magnetic equator and an amplitude threshold for emission triggering. In this model the direct transmitter pulse is too low in amplitude to trigger emissions, but due to the wave growth near the equator, subsequent echoes eventually reach the amplitude level required for triggering to occur. In many natural events a bandwidth restriction also appears to come into play since triggering only occurs when the signal bandwidth is sufficiently narrow. This bandwidth restriction may be related to the emission suppression effect [Raghuram et al., 1978] in which the emission-triggering abilty of ducted Siple transmitter signals decreases as the signal bandwidth increases.

The new type of triggered emission depicted in Figure 10 is unusual in a number of respects. For instance, this type of broadband hiss-like emission has never previously been observed to be triggered below the triggering wave frequency, although somewhat similar noise bands of shorter duration have occasionally been observed on satellites [Bell et al., 1981]. The long duration of the hiss-like emissions (~15 s) is also unusual. ASEs generally endure only for a few seconds. It is reasonable to assume that the long duration of the hiss-like emissions is not produced by wave echoing on L shells near $L \sim 4$ since none of the transmitter pulses in the same frequency range as the emission gives evidence of whistler-mode echoing. Thus the duration of the emission most probably is a reflection of the time constant of the emission mechanism.

Taken as a whole, the data suggest that a transmitter pulse has somehow triggered a mechanism for producing VLF hiss, but the hiss is not self-sustaining and eventually dies out. It is not clear whether the hiss was triggered by ducted or nonducted components of the transmitted signals. The fact that the hiss is triggered more than one second after the arrival of the leading edge of the associated transmitter signal suggests that the hiss may have propagated entirely in the nonducted mode after generation. If this is true we would expect that the hiss would not be observed on the ground at Roberval. Unfortunately, this point could not be checked since simultaneous data were not acquired at Roberval during the time that the emissions were observed on the satellite.

Appendix: August 15 Events

The ASE events of August 15 occurred within a complex framework of wave propagation phenomena. As demonstrated in Figure 8, strong whistler-mode echoing of both transmitter signals and natural signals was observed before, during and after the interval of emission triggering.

As discussed in the text, this echoing could not have taken place in either the ducted or nonducted modes near the satellite location at

L ~ 4.6. Consequently, the longer time delay signals seen on the satellite must have echoed on a lower L shell and must have reached the satellite only after having been scattered from the L shell of echoing.

Echoing phenomena existing in the natural wave background is shown in Figure 8b, as observed simultaneously at Palmer Station and on the satellite. These data are typical of those observed during the satellite pass. The lower panel of Figure 8b shows the existence of two separate whistler groups, W_1 and W_2. The arrival time at 5 kHz of each group is denoted by an arrow on the time axis, labeled 'W_1' and 'W_2,' respectively. The position of the causative atmospheric associated with the first W_1 group is indicated by the letter 'S' on the time axis. Group W_1 consists entirely of a number of whistlers that have propagated on magnetic shells near L ~ 3, and in this group there is no evidence of whistler traces corresponding to propagation on higher L shells. In addition, there is no evidence that any of the observed whistlers subsequently echo between hemispheres. In contrast to group W_1, group W_2 consists mainly of whistlers that have propagated on magnetic shells near L = 4, with only a single path in evidence near L ~ 3. Furthermore, most of the whistlers in the W_2 group are accompanied by VLF emissions triggered near the upper cutoff frequency of each whistler trace, and subsequently the W_2 whistlers can be seen echoing between hemispheres with a period of roughly 2.5 s.

The upper panel of Figure 8b shows simultaneous wave data acquired on the satellite. Two whistler traces are in evidence in this panel, with their arrival time at 5 kHz denoted by arrows labeled 'W_S.' There is a one-to-one correlation between whistler groups W_1 and W_S, while the group W_2 has no counterpart in the satellite data. Associated with each satellite whistler trace W_S is a noise burst near 5 kHz that occurs approximately 2 s after the W_S trace, and then proceeds to echo with a period of approximately 3.4 s. These noise bursts are very similar to those triggered by ducted whistlers that propagate just outside the plasmapause boundary [Carpenter, 1978].

The constant echo period of the echo trains of Figure 8b is a characteristic exhibited only in ducted propagation. Nonducted waves, in general, exhibit a variable echo period which increases with echo number [Edgar, 1976]. Thus it can be assumed that the wave packets comprising the echo trains have echoed within a duct before reaching the satellite. However, there are a number of reasons that imply that the satellite was not located within this duct at the time of the observations. First, the ground-to-satellite time delay (1.3 s) of the whistler components at 5.5 kHz was not equal to one-half of the period between echoes as it would be in a duct (1.3 s $\neq$ 1.7 s). Second, the time delay at the satellite between the initial whistler and the first echo was not equal to the period between echoes (1.5 s $\neq$ 3.4 s). Third, the period between echoes (~3.4 s) was about twice as large as the one-hop time delays usually observed on these magnetic shells ($4.0 \leq L \leq 4.3$) for ducted propagation.

One straightforward explanation of these observations is the following. The initial lightning flash on the earth's surface in the northern hemisphere injects wave energy into both ducted and nonducted modes of whistler propagation. The whistler W_S which first arrives at the satellite propagates via a nonducted raypath [Angerami, 1970; Bell et al., 1981]. The ducted whistlers propagate toward the southern hemisphere along one or more whistler-mode ducts near the L shell of the satellite. Somewhere near the magnetic equatorial plane, one or more of the ducted whistlers triggers VLF emissions at a frequency near the upper cutoff frequency of the whistler. Subsequently, this ducted whistler reaches the ionosphere in the southern hemisphere, where reflection occurs and where density irregularities scatter a small fraction of the whistler (and triggered emission) wave energy up to the satellite location. The bulk of the wave energy reenters the duct and echoes between hemispheres, with additional scattering to the sayellite taking place each time the echoing wave packet encounters the irregularities in the southern hemisphere.

The differences between groups W_1 and W_2 can be explained by hypothesizing that two centers of lightning activity exist in the northern hemisphere, one to the east (W_1) and one to the west (W_2) of the Siple/Roberval meridian. The whistler duct locations near the easternmost lightning center are mainly near L ~ 3, while those near the other center are mainly near L ~ 4. The centers are far enough apart (>1000 km) so that lightning from one center does not excite ducts near the other center. Figure 8c shows in more detail a W_2 whistler group and accompanying echo train. The approximate location of the causative atmospheric is at the point labeled '0' on the time axis. Arrival times of the first 3 echoes are labeled 'E_1,' 'E_2,' and 'E_3,' respectively. In all, at least 8 two-hop echoes can be seen.

The time delay at 5 kHz of the W_2 whistlers that triggered emissions lay in the range 1.2-1.7 s. One prominent trace that triggered emissions between 5-5.5 kHz was inferred to be located near L = 4.3. This trace was observed to have a time delay of 1.2 ± 0.1 s at 5.5 kHz, which was approximately its upper cutoff frequency.

It is reasonable to assume that the longer time delay transmitter signals of Figures 7 and 8a have echoed in the same ducts as those in which the noise bursts of Figure 8b have echoed. However, the lack of a high L shell whistler trace in the W_2 groups make a direct determination of the duct location impossible. Making the plausible assumption that the noise bursts were triggered near the upper cutoff frequency of the direct ducted whistlers, we can estimate the equatorial gyrofrequency in the duct to be ~11 kHz and L ~ 4.3. On the other hand, it cannot be completely ruled out that the transmitter signals are echoing on one or more of the ducts that guide the W_2 groups, possibly the duct near L ~ 4.3 related to one of the prominent whistler traces.

Given that the longer time delay transmitter signals have echoed in the same ducts as the echoing noise bursts, it is reasonable to as-

sume that these signals arrive at the satellite in a manner analogous to that of the noise burst echoes. That is, we assume that a portion of the wave energy from the transmitter is injected into both ducted and nonducted modes of whistler propagation. The signals that first arrive at the satellite propagate via a direct nonducted raypath from the south. Ray tracing studies using commonly accepted models of the magnetosphere show that the measured group time delay (~1.8 s) of the direct signal is consistent with this interpretation. The ducted signals propagate toward the northern hemisphere, along one or more whistler-mode ducts near the L shell of the satellite, reflect and subsequently reach the ionosphere in the southern hemisphere, where reflection occurs again and where density irregularities scatter a small fraction of the ducted signal (and any triggered emission) up to the satellite location. The bulk of the wave energy reenters the duct and continues to echo between hemispheres, with additional scattering to the satellite taking place each time the echoing wave packet encounters the irregularities in the southern hemisphere.

A sketch of the model we propose is shown in Figure 9. If this model is correct then the longer-time delay wave train that follows each direct nonducted transmitter pulse should have a minimum time delay (at ~5 kHz) with respect to this pulse of $\Delta t = t_2 + t_S - t_N$, where t_2 is the smallest two-hop time delay associated with the excited ducts, t_S is the group time delay of the scattered signals from the ionosphere to the satellite, and t_N is the group time delay of the direct nonducted signal.

According to our model, $t_2 \approx 3.4$ s, and if we assume $t_S \sim t_N$, then $\Delta t \sim 3.4$ s. Measurements indicate that $\Delta t \approx 3.0$-3.5 s. Thus the model gives reasonable agreement with observations. Measurements indicate that the maximum value of t_2 for the excited ducts was approximately 4 s. Since the duration of the triggering pulses was 1 s, our model predicts that any ASE occurring more than 5 s after the arrival of the longer-time delay wave train must have been triggered by an echo of the ducted one-hop signal. With this criterion, the ASE shown in Figure 7a would have been triggered by echoes of the original one-hop signal, while that of Figure 7b would have been triggered by either the one-hop or two-hop signals.

The continuous nature of the longer time delay wave trains can be explained by taking into account the differing two-hop time delays among the excited whistler ducts and by postulating the existence of coupling between these ducts [Smith and Carpenter, 1982].

Acknowledgments. This work has profited greatly from numerous discussions with our colleagues in the Radioscience Laboratory during the course of this work, in particular R. A. Helliwell and D. L. Carpenter. The invaluable aid of J. Katsufrakis in setting up the real time data monitoring network is gratefully acknowledged. The final manuscript was typed by K. Dean and K. Faes. Analysis of the EXOS-B wave data was sponsored by the National Aeronautics and Space Administration under contract NGL-05-020-008. Data acquisition at Siple, Roberval, and Palmer Stations was supported by the Division of Polar Programs of the National Science Foundation under grants DPP80-22282 and DPP80-22540. The joint experiment was made possible through the Grant-in-Aid for Overseas Scientific Survey of the Japanese Ministry of Education, Science and Culture.

The Editor thanks N. R. Thomson and H. C. Koons for their assistance in evaluating this paper.

References

Angerami, J. J., Whistler duct properties deduced from VLF observations made with the OGO 3 satellite near the magnetic equator, J. Geophys. Res., 75, 6115, 1970.

Bell, T. F., U. S. Inan, and R. A. Helliwell, Nonducted coherent VLF waves and associated triggered emissions observed on the ISEE 1 satellite, J. Geophys. Res., 86, 4649, 1981.

Bernard, L. C., A new nose extension method for whistlers, J. Atmos. Terr. Phys., 35, 871, 1973.

Carpenter, D. L., Whistlers and VLF noises propagating just outside the plasmapause, J. Geophys. Res., 83, 45, 1978.

Carpenter, D. L., and T. R. Miller, Ducted magnetospheric propagation of signals from the Siple, Antarctica, VLF transmitter, J. Geophys. Res., 81, 2692, 1976.

Dowden, R. L., A. C. McKay, L. E. S. Amon, H. C. Koons, and M. Dazey, Linear and nonlinear amplification in the magnetosphere during a 6.6-kHz transmission, J. Geophys. Res., 83, 169, 1978.

Edgar, B. C., The upper- and lower-frequency cutoffs of magnetospherically reflected whistlers, J. Geophys. Res., 81, 3327, 1976.

Helliwell, R. A., and J. P. Katsufrakis, VLF wave-injection experiments into the magnetosphere from Siple Station, Antarctica, J. Geophys. Res., 79, 2571, 1974.

Helliwell, R. A., D. L. Carpenter, and T. R. Miller, Power threshold for growth of coherent VLF signals in the magnetosphere, J. Geophys. Res., 85, 3360, 1980.

Inan, U. S., T. F. Bell, D. L. Carpenter, and R. R. Anderson, Explorer 45 and IMP 6 observations in the magnetosphere of injected waves from the Siple Station VLF transmitter, J. Geophys. Res., 82, 1177, 1977.

Kimura, I., H. Matsumoto, T. Mukai, K. Hashimoto, R. A. Helliwell, T. F. Bell, U. S. Inan, and J. P. Katsufrakis, Jikiken (EXOS-B) observation of Siple transmissions, Adv. Space Res., 1, 197, 1981.

Kimura, I., H. Matsumoto, T. Mukai, K. Hashimoto, M. Morikura, T. F. Bell, U. S. Inan, R. A. Helliwell, and J. P. Katsufrakis, EXOS-B/Siple Station VLF wave-particle interaction experiments, 1., General description and wave-particle correlation, J. Geophys. Res., this issue.

McPherson, D. A., H. C. Koons, M. H. Dazey, R. L. Dowden, L. E. S. Amon, and N. R. Thomson, Conjugate magnetospheric transmissions at VLF from Alaska to New Zealand, J. Geophys. Res., 79, 1555, 1974.

Park, C. G., and R. A. Helliwell, Magnetospheric effects of power line radiation, Science, 200, 727, 1978.

Raghuram, R., T. F. Bell, R. A. Helliwell, and

J. P. Katsufrakis, Echo-induced suppression of coherent VLF transmitter signals in the magnetosphere, J. Geophys. Res., 82, 2787, 1977.

Smith, A. J., and D. L. Carpenter, Echoing mixed-path whistlers near the dawn plasmapause, observed by direction-finding receivers at two Antarctic stations, J. Atmos. Terr. Phys., in press, 1982.

(Received December 21, 1981;
revised June 4, 1982;
accepted June 22, 1982.)